Article:

Hussein, D, Rashid, F, Lawrence, JA et al. (2 more authors) (2022) Influence of fractures on the reservoir quality of Lower Miocene carbonates in Northern Iraq. Arabian Journal of Geosciences, 15 (1). 63. ISSN 1866-7511

https://doi.org/10.1007/s12517-021-09345-9

Influence of fractures on the reservoir quality of Lower Miocene carbonates in Northern Iraq

Devan Hussein[1*], Fraidoon Rashid[2], James A. Lawrence[3], Paul W.J. Glover [4] and Piroska Lorinczi[4]

[1] University of Sulaimani, Department of Geology, Kurdistan, Iraq.
[2] Kurdistan Institution for Strategic Study and Scientific Research, Sulaimani, Iraq.
[3] Department of Civil and Environmental Engineering, Imperial College, London, UK.
[4] School of Earth and Environment, University of Leeds, Leeds, UK.
*Corresponding author, email: devan.hussein@univsul.edu.iq

Abstract

The Zagros Fold and Thrust belt of the Kurdistan region of northern Iraq hosts major volumes of hydrocarbons in multiple fractured carbonate reservoirs throughout the Jurassic, Cretaceous, Palaeogene and Neogene. Limited research has been undertaken to characterise these recently discovered carbonate reservoir rocks. Here, the reservoir quality of the Neogene Euphrates and Jeribe Formations are investigated. Samples from five outcrops along the Azhdagh and Mamlaha anticlines and from four nearby wells (North Oil Company wells JM37, KM3, SAR1 and KU1) have been analysed to understand better their reservoir properties. In both formations very low matrix porosities (<12±0.5%) were measured and no visible pore connectivity was observed in thin sections. Matrix permeability was less than 0.10±0.008 mD. The low porosity of the Euphrates and Jeribe Formation carbonates is related to diagenetic modifications including intense cementation and compaction. Given the low matrix porosity and permeability, the effect of fractures on fluid flow was investigated as a possible mechanism for enhanced reservoir quality. Naturally fractured core samples and highly fractured outcrops for both formations demonstrated enhanced flow of more than three orders of magnitude compared to matrix permeability. Lateral heterogeneities were observed in the area under investigation with lower fracture porosity and permeability in the North East compared to the South West of the region. Outcrop fractures were investigated near to the wells on the flanks of the basin. The fracture network was found to be composed of two sets of sub-vertical, perpendicular fracture sets and sub-horizontal bedding. The fractures were closely spaced, persistent, with wide apertures rough surfaces and very well interconnected. The permeability data combined with field fracture survey information provides evidence that the reservoir quality in the drilled wells must in part be a result of a permeable well-interconnected fracture network.

Key words: Fractures; Carbonate reservoirs; Porosity; Permeability; Reservoir Quality; Diagenesis

INTRODUCTION

More than half of the world's proven hydrocarbon resources are located in carbonate reservoirs (Dou et al., 2011; Garland et al., 2012), the great majority of which would not be commercially viable without either extensive natural fractures (Nelson, 1985; Yuan et al., 2004; Liu et al., 2008; Mu et al., 2009; Zeng et al., 2010; Zhou et al., 2003; Khoshbakht et al., 2012; Kosari et al., 2017; Bisdom et al., 2017) or the generation of artificial fracture networks by hydraulic fracturing (Olson and Dahi-Taleghani, 2009).

This study investigates reservoir quality variations of the carbonate formations enhanced by natural fracturing and/or modified by diagenesis including dolomitization and dissolution. The impact of natural fracturing of the Euphrates and Jeribe formations in Iraqi Kurdistan has been quantified using outcrop fracture measurements as well as laboratory testing of core material obtained from wells and outcrops. The investigation was located in Zagros Fold and Thrust belt of the Kurdistan within the central and basinal locations in the Kirkuk embayment (Figure 1).

This work considers how the rock mass properties (porosity, permeability, fracturing) affect the potential reservoir quality and builds on the work of Hussein et al. (2017) and Hussein et al., (2018) to consider this within the context of the existing formation and the relationships between the microfacies. In doing so interesting lateral variations are also identified. An overview of fracturing in carbonates is given followed by a section on the regional geological setting to provide a comprehensive background, prior to the methodologies and the results in these carbonate reservoir being considered.

The novelty of this work resides in the fact that this is the first time that a combination of geological, geomechanical and petrophysical approaches have been used to analyse the causes and implications of fracturing in the studied form Euphrates and Jeribe formations, with account also being taken of concomitant diagenesis and its influence on reservoir quality.

There has been extensive research into the dual porosity systems (Haghi et al., 2018), which fractured carbonate reservoirs represent (Nelson, 2001; Agosta et al., 2010; Volatili et al., 2019). The development of natural fracture networks in reservoir rocks depends on many factors but most fundamentally on the interplay between the mechanical properties of the unfractured rock, the local stress tensor, and the subsequent evolution of the mechanical properties as the rock becomes fractured (Graham et al., 2003; Agosta and Aydin, 2006; Micarelli et al., 2005; Antonellini et al., 2008; Rustichelli et al., 2013a; Fossen, 2016). The stress tensor can promote fracturing but may also lead to fracture closure and sealing (Nelson, 2001) depending on the orientation of the major stress direction, and may also result in the formation of other structures such as stylolites (Yu et al., 2018; Croize et al., 2010; Fossen et al., 2011).

The linked evolution of the mechanical properties and the stress tensor controls the style and the extent of fracturing (Antonellini et al., 2008). However, fracture characteristics such as aperture, persistence spacing and the roughness of fracture surfaces are all known to follow fractal distributions (Micarelli et al., 2006; Agosta et al., 2010). Such fractal behaviour commonly extends over many orders of magnitude, in carbonate fractures scale from microfractures (Zhou et al., 2006) which can be microns in length, to large-scale faults which may even extend kilometres even beyond the boundaries of reservoir units (Zambrano et al., 2016). Such scaling behaviour is exhibited as a power-law distribution which shows that many more low-persistence (short), small-aperture fractures occur than larger-scale ones.

The process of fracturing affects both the porosity of the rock, and the efficiency of fluid flowing through it. Fracture porosity usually has only a slight positive impact on the total porosity compared to the porosity provided by the inter-granular pores of the matrix (Nelson, 2001). However, the connectivity of fractures can lead to increases in permeability by many orders of magnitude, more than would be the case if the same porosity increase took the form of intergranular pores or vugs. However, in terms of reservoir management, the direct and effective transport of fluids along fracture conduits can cause difficulties. It is relatively quick and easy to produce oil from a natural fracture network (Volatili et al., 2019), but once this is exhausted the fractures may fill with water unless care is taken, and then it will become impossible to produce oil from the pore systems in the blocks of rock between the fractures. If the fractures are closed, they can effectively compartmentalise the reservoir, offering even greater challenges for the reservoir engineer (e.g., Tondi et al., 2016).

The directionality of fracture sets is generally defined by the local stress tensor (Peacock et al., 2018). This lends an anisotropy to the flow properties of the reservoir (Kazemi et al., 1976), affecting optimal fluid flow and having implications for the placement of production and injection wells, as well as constraining enhanced oil recovery (EOR) and reservoir stimulation design (Jolley et al., 2007).

Petrophysical evaluation of fractured reservoirs consists of assessing the rock matrix porosity and permeability alongside fracture porosity and permeability (connectivity) to provide a holistic understanding of the behaviour of the rock mass (Ahr, 2008). Fractures generally enhance reservoir quality by providing a small increase in porosity, but more importantly by increasing permeability often by at least an order of magnitude (Laubach, 2003; Barr et al., 2007; Agosta et al., 2010; Korneva et al., 2014; Rashid et al., 2015a; 2015b; 2017; Dashti et al., 2018; Rashid et al., 2020). The improved reservoir permeability quality depends on the intensity, orientation, aperture and persistence of fractures and on how inter-connected they are.

GEOLOGICAL SETTING

In this study, we investigate the Lower Miocene Euphrates and Jeribe Formations which are considered to be the principal reservoirs and most important exploration targets in the Cenozoic petroleum system in the Kurdistan region of NE Iraq (Aqrawi et al., 2010 and Western Zagros Final Well Reports 2011), tectonically within the Low Folded Zone (LFZ) of the Iraqi main tectonic segments, which is characterized by the presence of NW-SE trending low amplitude folds separated by relatively wide synclines (Jassim and Goff, 2006). The Zagros Fold and Thrust Belt in Iraqi Kurdistan are characterized by multiple petroleum systems with a wide range of producing and potential reservoirs (Figure 1) (Aqrawi et al., 2010; Jassim and Goff, 2006). Reservoir units are present in the Triassic, Jurassic and Cretaceous intervals, but the most producible reserves in the region occur in the Lower Miocene Euphrates and Jeribe Formations (Figure 2). The study area forms the NE region of the Kormor, Sarqala and Kurdamir anticlines in Kurdistan. Both formations are composed of inner-shelf carbonates with both primary matrix porosity and secondary porosity due to dolomitization (Jassim and Goff, 2006, Aqrawi et al., 2010; Hussein et al., 2017). The Euphrates Formation is underlined by Oligocene formations and separated from Jeribe Formation by Dhiban Formation. Both formations are occasionally contiguous without the Dhiban interlayer. The Jeribe Formation is covered by red clay stone Formation of the Fatha formation (Hussein et al., 2017). Hussein et al. (2018) identified a diverse range of pore types including intercrystalline, interparticle, moldic and vuggy pore space from grain-dominated and mud-dominated fabrics along with different pore sizes and pore size distributions (Hussein et al., 2018).

Buday (1980) indicated that the Euphrates Limestone formation was deposited under shallow marine, reef and lagoonal conditions. Its facies include fossiliferous packstones of benthonic foraminifera with gastropod, algae and a non-skeletal component of oolites and pellets (Al-Juboury et al., 2007).

The Euphrates Formation is a well-bedded limestone with occasional anhydrite in some subsurface sections, which may be tongues of the Ghar and Dhiban Formations (Jassim and Goff, 2006). The greatest measured thicknesses of the Euphrates Formation (80 m and 90 m) occur in the Hamrine and Ajeel oil fields, respectively (Hussein et al., 2017). However, according to van Bellen et al. (1959), the type locality of the Euphrates Formation is near Wadi Fuhaimi, where it is only 8 m thick, subsequently more expanded, stratigraphically complete, representative sections have been described.

The formation unconformably overlies Oligocene and Eocene formations, but the upper boundary is often not exposed as in the type locality (Jassim and Goff, 2006). The investigation of the Euphrates

Formation in the Kurdistan region revealed that the Euphrates Formation is overlain by anhydrites of the Dhiban Formation.

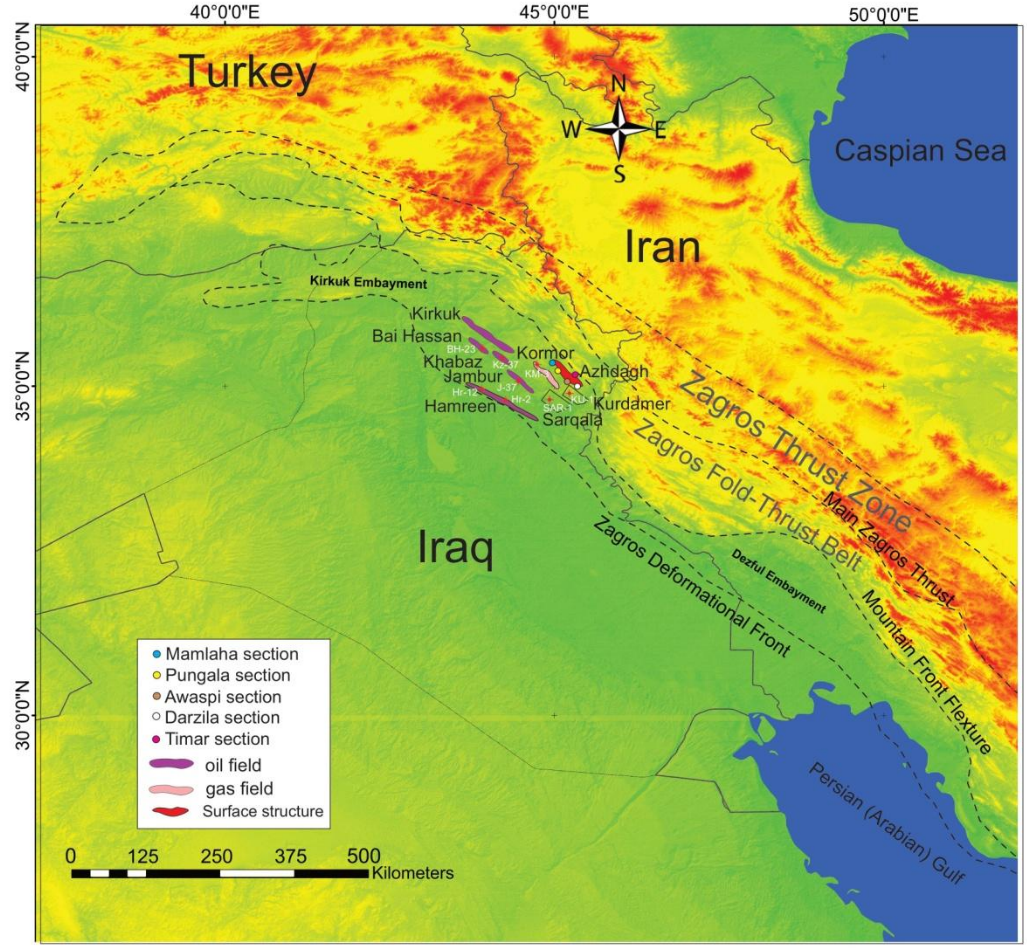

Figure 1 Geological map of the Kurdistan region and north-east of Iraq showing the selected fields, boreholes (borehole codes in red cross), blocks (in red cross), outcrop sections (names in colour circles) of the study area, base map modified from (Sissakian et al., 2000).

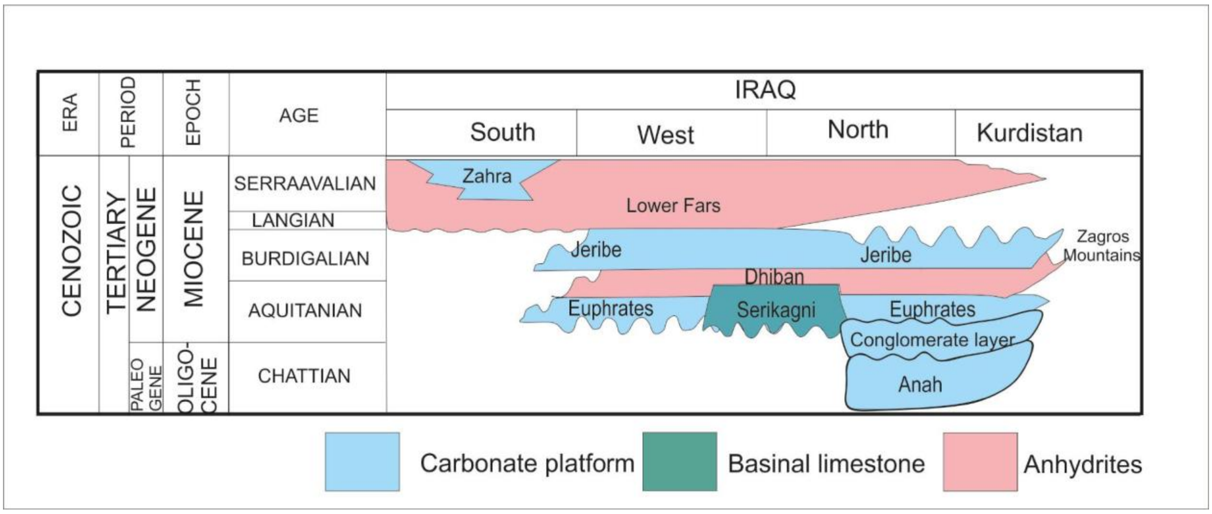

Figure 2 Chronostratigraphic chart of Iraq (modified and redrawn after Petroleum Geo-service (2000).

The Jeribe Formation is of Burdigalian age (Figure 2). The Jeribe Limestone Formation near Jaddala village in the Sinjar anticline was described by van Bellen in 1957 as having thickness of 70 m, and consisting of recrystallized, dolomitized limestones (van Bellen, 1975), where a thickness of 73 m of limestone is recorded (Hussein et al., 2017). In well sections it comprises argillaceous limestones and anhydrites. The lower contact is unconformable with the Serkagni Formation in the type area, and in many areas a conglomeratic bed occurs at the base of the Jeribe Formation, or it passes gradationally into the overlying Fatha (Lower Fars) Formation (Jassim and Goff, 2006).

Aqrawi et al. (2010) has indicated that the Jeribe Formation was deposited uniformly throughout the basin. In the basin centre, cycles of porous open marine carbonates are interbedded with relatively tight restricted marine carbonates and evaporites. It represents an upward shallowing carbonate ramp sequence. Previous authors have investigated the structural geology and sequence stratigraphy however no previous work has focused on the fractures, their origin, distribution and properties and how these affect carbonate reservoirs quality. A detailed microfacies and stratigraphic study was undertaken from observations of outcrops, cores and well logs, most documented microfacies in both formations show shallowing upwards cycles from north-east to south-west of gradual depositional gradient, where complete depositional cycles being preserved towards the basin centre to the south-west (Hussein et al., 2017).

METHODOLOGY

Samples for petrophysical analysis were selected from five outcrop sections at Darzila (35°08’N 45°17’E), Awaspi (35°09’N 45°31’E), Timar (35°23’N 45°22’E), Mamlaha (34°53’N 43°53’E) and Pungala (35°01’N 45°35’E) and 10 drilled wells in the Kormor (35°24’N 44°49’E), Bai Hassan (35°36’N 44°4’E), Khabaz (35°33’N 44° 39'E), Pulkhana (35° 35’N 44°32’E) and Hamrine (34°58’N 43°47’E) fields, which are shown as crossed green circles in Figure 1, together with their codes. Rock samples were collected from outcrop sections, whilst core and cutting samples were provided by the North Oil Company (NOC) from the subsurface sections (drilled wells), as well as wireline well logs and crude oil samples. A total of 62 core samples were used to undertake 396 porosity and/or permeability measurements (Table 1).

Laboratory measurements of porosity, permeability, electrical resistivity (AC frequency = 1 kHz, applied potential difference = 1 V), NMR spectra and capillary pressure curves were conducted on samples from the Euphrates and Jeribe Formations (Hussein et al., 2018). First the core samples were dried in an oven at a temperature of 60°C for 72 hours to remove formation fluids in the pore spaces before starting routine core analysis. A helium porosimeter was used to measure the porosity of the samples.

The same group of plug samples were then used for measuring Klinkenberg-corrected matrix permeability (Klinkenberg, 1941; Rushing et al., 2004; Tanikawa and Shimamoto, 2006; Haines et al., 2016). Steady-state gas permeability using helium as the process gas (Ross, 2011) was carried out on all samples with a porosity greater than 12%. It was considered that samples with porosity less than 12% would not give accurate permeability results when applying the steady-state technique (Rashid et al., 2015a; 2015b; 2017). Consequently, a helium pulse-decay permeametry was used for on all samples with porosity less than 12%.

Fracture data were collected from surface outcrops at Darzila (Figure 1). Lower Miocene Euphrates and Jeribe Formations fracture measurements were taken at outcrop using the scan line method where fracture data is systematically collected in an *x*, *y* and *z* orientation, recording fracture type, orientation, dip, spacing, aperture and nature of filling, consistency of infilling and roughness (Table 2) (Rustichelli et al., 2016; Miranda et al., 2018). Hemisphere stereonet pole plots have been made with Rocscience dips 6.0® software in order to show the dip direction of bedding joints and fractures. The fracture measurements were integrated with sedimentological data, conventional wireline logs and core analysis data to characterise the combined impact of fracturing on reservoir quality (Nelson, 1985; Laubach et al., 2009; Hou and Pan, 2013; Bisdom et al., 2017). This is the first time that the synthesis of this data has been carried out for the formations studied in this paper.

The Lower Miocene Euphrates and Jeribe Formations were observed throughout the outcrop sections studied, and lithological variations and sedimentological characteristics were recorded by careful logging. A micro-structural analysis was carried out on the outcrops and the collected data were described and then numerically analysed. Structures recorded were of both sedimentary and tectonic origin; the former comprise sedimentary stylolites, while the latter were documented as tectonic fractures.

Wireline logging and particularly image logs would have provided extremely useful adjunct data for a study such as that described in this paper. Unfortunately such data was not available to us. Relevant petrophysical, microfacies and depositional environment data from Hussein et al. (2017) and Hussein et al. (2018) have also been used in this paper in order that the wider implications of the effect of fractures may be discussed fully.

Table 1 Number of core plugs in the Euphrates and Jeribe Formations from studied wells (Figure 1). ϕ porosity; *k* permeability

Wells	No. of cores (Euphrates Fm.)	No. of cores (Jeribe Fm.)	No. of data from NOC (Euphrates Fm.)	No. of data from NOC (Jeribe Fm.)
HR-2	5	16	131 ($\phi$and k)ØandK)	23 (ϕonly)
BH-23	-	2	-	
PU-7	3	-	-	
JM-37	6	-		46 (ϕonly)
KM-3	3	9	79 (ϕonly)	17 ($\phi$and k)
Outcrops	9	7	-	-

Table 2 Standard fracture data collection methodologies

Types	Aperture	Nature of filling	Consistency of infilling		Roughness
0 Fault zone	1 Wide (>200 mm)	1 Clean	Soil strength	Rock strength	1 Polished
1 Fault	2 Mod. wide (60-200 mm)	2 Surface staining	1 Soft	5 Weak	2 Slickenside
2 joint	3 Mod. Narrow (20-60 mm)	3 Non-cohesive	2 Film	6 Mod. Strong	3 Smooth
3 Cleavage	4 narrow(6-20 mm)	4 Cohesive	3 Stuff	7 strong	4 Rough
4 Schistosity	5 Very narrow(2-6 mm)	5 Cemented	4 Hard	8 Very strong	5 Defined side
5 shear	6 Exl. narrow (<2 mm)	6 Calcite			6 Small slope
6 Fissure	7 Tight	7 Chlorite, talc			7 Very rough
7 Tension crack		8 Others			
8 Foliation					
9 Bedding					

RESULTS

Fractures measured at outcrop

The main types of fractures that were observed at the Darzila section in the Euphrates Formation are joints and bedding surfaces (Figure 3). Their persistence ranges between 0.3 m to over 3 m, with master joints having persistence greater than the exposure and dipping into the ground. The fracture frequency was 300 mm and exhibited clean, rough surfaces with apertures varying from 0-7 mm to 4 mm wide. Two distinct joint set orientations were identified, these were sub-vertical and perpendicular to each other (Figure 3). One fracture set trending 090/81 S and the second 177/81 W, with the bedding orientation trending 134/05 SW as shown in Figure 4.

Fractures in the Jeribe Formation at the Darzila section consist of narrow, clean, rough joints, their persistence ranging from 0.3 m to greater than 3 m. The fracture frequency 230 mm with apertures varying from 0-7 mm to 6.4 mm wide. Discontinuous incipient joints developed between bedding planes in some cases these have been cut by persistent master joints as shown in Figure 5. The general orientation of fracture sets and bedding in the Jeribe Formation indicates a network of two dominating fracture sets which are sub-perpendicular to each other and sub-vertical. One fracture set has orientation 082/81 S and the second fracture set has orientation of 165/80 W, with the bedding orientation 134/13 SW (Figure 6).

Figure 3 The expression of fractures at the outcrop sections. (A) Fracture (joint) sets in the Euphrates Formation; with annotated joint plane directions and definitions. (B) Fracture sets in the Euphrates

Formation; forming a blocky pavement structure the red box represents scale, while the purple arrows show the main joint sets.

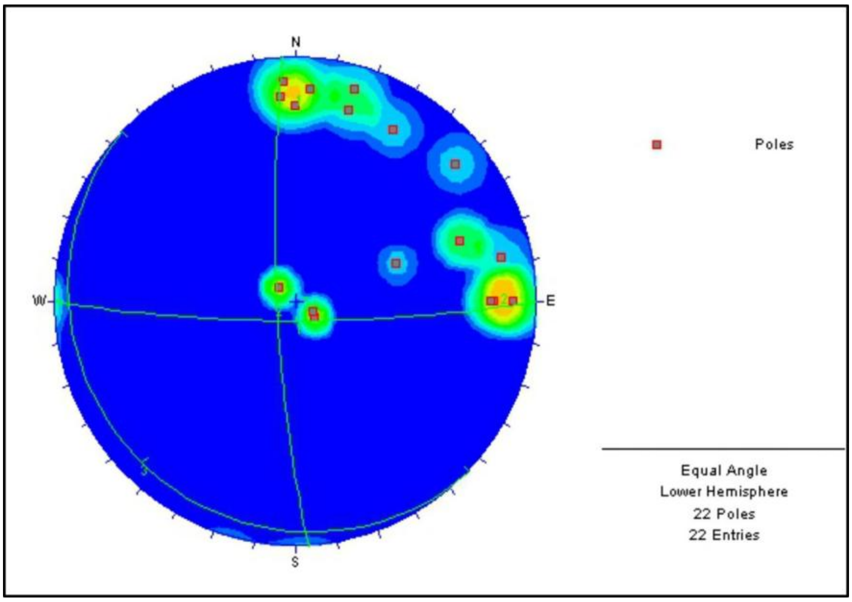

Figure 4 Stereonet diagram showing the fracture orientation of the Euphrates Formation, Darzila section made using Rocscience dip 6® software.

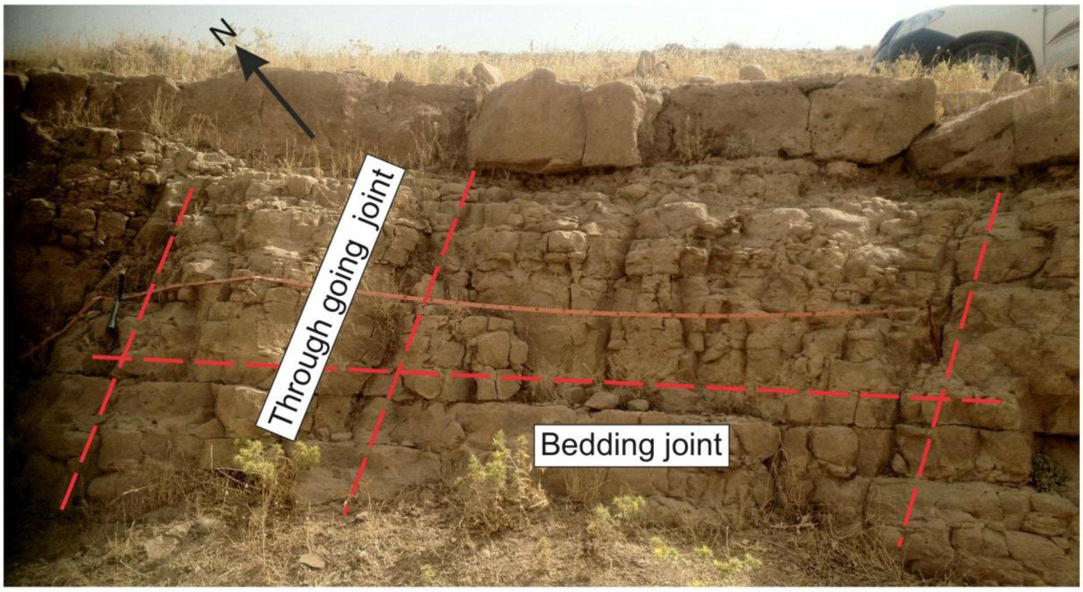

Figure 5 Fracture types, including bedding joints and through-going joints in the Jeribe Formation, Darzila section.

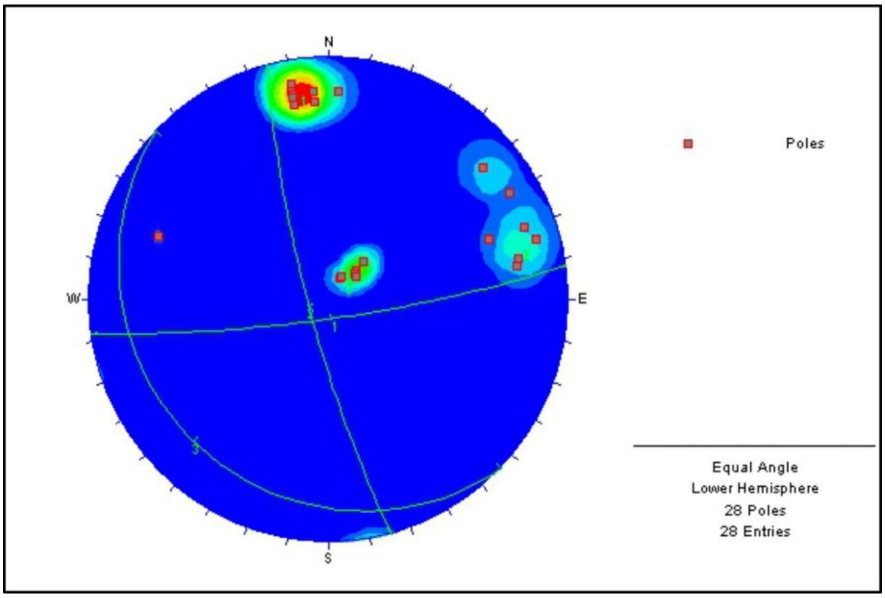

Figure 6 Stereonet diagram showing the fracture orientations in the Jeribe Formation, Darzila section made using Rocscience dip 6® software.

Core plug porosity

The helium porosity of the collected core plugs from the Euphrates and Jeribe Formation was measured and results are shown in Table 5 and Table 6, which show that the study region contains a clear division in porosity behaviour between the NE and SW of the study region. The measured helium porosity of the Euphrates Formation from the outcrop sections and subsurface core samples in the NE part of the studied area ranges from 1.4±0.5% to 11.68±0.5%, with an arithmetic mean of 6.36%. Please note that for these values and subsequent values of the same type (i) the uncertainties in each of the low and high values defining a range are the experimental errors in those values, while (ii) the uncertainties in arithmetic mean values represent the spread of the values in the population of measurements used to make the arithmetic mean and represent the standard deviation of that population. In the samples from the SW of the study area, the porosity from the subsurface core samples from well HR2 ranged from 7.7±0.5% to as high as 26.6±0.5%, with an arithmetic mean of 17.4%. Helium porosity in the Euphrates Formation varies widely across the study area (Figure 7A).

Significant increases of porosity were recorded in the Jeribe Formation samples in the SW part of the studied area compared to the NE region (Figure 7B). The porosity ranged from 4.4±0.5% to 37.7±0.5%, with an arithmetic mean of 24.16% in well HR2, but porosity was reduced to 0.2±0.5% to 8.4±0.5%, with an arithmetic mean of 2.15% in well KM3 and outcrop sections of the NW part of the study area.

Table 3 Fracture data of the Euphrates Formation

Section	No	Type	Dip	Dip direction	Persistence (cm)	Aperture	Infilling	Roughness
X	5	2	82	184	30	3	1	4
	45	2	84	270	250	7	1	4
	22	2	80	176	300			4
	190	2	84	270	>300	1	1	4
	225	2	79	270	150			4
	235	2	78	270	30	7	1	4
	237	2	77	180	150			4
	260	9	72	250	120	7	7	4
	300x	9	72	250	250	4	1	4
Y	95y	2	12	310	40	7	1	4
	120	2	12	310	40	7	1	4
	140	2	82	230	20	7	1	4
	170	2	48	250	25	7	1	4
	200	2	10	300	>300	5	1	2
	215	9	10	130	>300		1	4
	230	9	10	130	>300		1	4
	245	9	10	130	>300		1	4
	260	9	10	226	>300	6	1	4
	270	9	10	226	>300	6	1	4
	300	9	10	226	>300	6	1	4
Z	10z	2	84	196	300	1	1	4
	45	2	78	210	150	1	1	4
	100	2	78	196	300	5	1	4
	140	2	82	258	80	4	1	4
	210	2	84	177	280	5	1	4

Table 4 Fracture data of the Jeribe Formation

Section	No	Type	Dip	Dip direction	Persistence (cm)	Aperture	Infilling	Roughness
X	5	2	81	170	150	4	1	4
	9	2	82	170	200	7	1	4
	25	2	82	240	25	7	1	4
	40	2	84	170	120	7	1	4
	45	2	84	170	70	7	1	4
	70	2	81	170	70	7	1	4
	75	2	77	260	0.5	7	1	4
	100	2	74	110	30	7	1	4
	102	2	81	176	130	7	1	4
	128	2	80	230	100	4	1	4
	150	2	71	250	100		1	4
	242	2	82	250	40	7	1	4
	248	2	81	176	80	7	1	4
	258	2	78	258	100	7	1	4
	270	2	84	254	50	7	1	4
	287	2	78	176	30	7	1	4
	294	2	78	170	0.5	7	1	4
	300x	2	80	170	100	7	1	4
Y	20y	9	11	210	300	7	1	4
	40	9	12	212	300	7	1	4
	70	9	24	224	>300	7	1	4
	80	9	24	224	>300	7	1	4
	100	9	24	224	>300	7	1	4
	130	9	19	225	120	7	1	4
	155	9	17	226	>300	7	1	4
	141	9	17	233	>300	7	1	4
	194	2	81	183	120	7	1	4
	195	2	80	230	100	7	1	4

Permeability measurements

The permeability of 66 core samples from the studied area in the surface and subsurface sections of the Lower Miocene carbonate formations was measured by steady-state and pulse decay gas permeametry. In addition, a recorded permeability data set was used from the final well test (Table 1) conducted by the North Oil Company of Iraq (NOC), Kirkuk. Based on the measured data sets of petrophysical analysis including porosity and permeability beside documented pore types in the studied formations two group of samples are recognized. Hussein et al. (2018) established that the Euphrates and Jeribe Formations are characterized by complex and heterogeneous pore systems on the basis of porosity values, types and texture. The measured data throughout the study area have various types of pores, different pore sizes, and pore size distribution. Diverse pore types were determined, such as intercrystalline, interparticle, moldic and vuggy pore space from grain-dominated and mud-dominated fabrics.

The results are presented as porosity-permeability cross-plots for the measured porosity and permeability data using core derived porosity (helium porosity) and measured Klinkenberg-corrected permeability (pulse decay and steady state).

In the first group the observed intercrystalline micropores have measured porosities which do not exceed 12±0.5%. The measured Klinkenberg-corrected matrix permeability_varied from 65±6.5 nD to 0.26±0.0.03 mD for the highly cemented samples of the Euphrates and Jeribe Formations in the north-eastern part of the study area. Calcite cement reduced the pore connectivity and destroyed permeability and fluid flow in this part of the area. An example of this is given in the upper panel of Figure 8, which shows a stained thin section from the Kormor well at a depth of 1552.30 m, showing ferroan spary calcite cements filling molds and vugs. The staining was carried out using (Dickson, 1965, 1966) technique, and the photomicrograph was imaged using a polarized petrological microscope with a camera.

Data points representing this pore type are confined to the bottom left-hand side of the poroperm plot (Figure 9). This relationship of poroperm data represents the measured data from the North-East of the studied area including the Kormor, Jambur and the outcrop sections. The fractured samples of this north-eastern group exhibit a large increase in the magnitude of permeability. We observed that fracture connectivity enhanced permeability by one order of magnitude in the Euphrates samples and by up to 3 orders of magnitude in the Jeribe Formation.

Table 5 Statistical parameters of the helium porosity measurements of the Lower Miocene Formations in the north-eastern part

Format-ion	Units In the north-eastern part	Microfacies	Helium porosity (%)			
			Mean	mode	Maximum	Minimum
Jeribe	U1	J4 and J6	3.0	0.6	8.2	0.2
	U2	J6	1.5	0.8	6.3	0.2
	U3		2.0	1.1	8.4	0.6
	U4		-	-	-	-
	U5		-	-	-	-
Euphrates	U1	E1, E3 and E4	7	6.5	11.9	2.1
	U2	E1	4.8	6	10.1	1.4

Table 6 Statistical parameters of the helium porosity measurements of the Lower Miocene Formations in the south-western part

Formation	Units In the south-western part	Microfacies	Helium porosity (%)			
			Mean	mode	Maximum	Minimum
Jeribe	U1		24.9	24	33	5.3
	U2	J6	22.04	32.8	33.7	4.4
	U3		26	30.9	35.2	11.1
	U4	J4	23.6	30	34	4.4
	U5	J3	25.1	22.4	37.2	7
Euphrates	U1	E1	17.9	16.8	22.66	5.62
	U2	-	-	-	-	-

The second pore group that can be recognised from the poroperm plot shown in Figure 9 is derived from dissolution and dolomitization that created intercrystalline mesopores, moldic and vuggy mesopores. Diagenetic processes have affected reservoir quality, increasing hydraulic connectivity and permeability significantly throughout the south-western part of the study area. In particular. dolomitization has increased the matrix permeability of the Euphrates Formation in the south-western part of the study area by one order of magnitude by comparison with the north-eastern region. In the Jeribe Formation diagenetic hydraulic conductivity enhancement increased the matrix permeability by 3 orders of magnitude and a maximum permeability of 172.6±8.6 mD was recorded, whereas a maximum permeability of 3.5±0.175 mD was recorded in the Euphrates Formation. The lower panel of Figure 8 shows an example of the microstructural changes that lead to enhanced porosities and permeabilities arising from dissolution. This photomicrograph is a stained thin section from the Jeribe Formation in well HR2, depth 494 m showing vuggy porosity created by dissolution, and an enlarged moldic porosity. The staining and imaging method were the same as described previously.

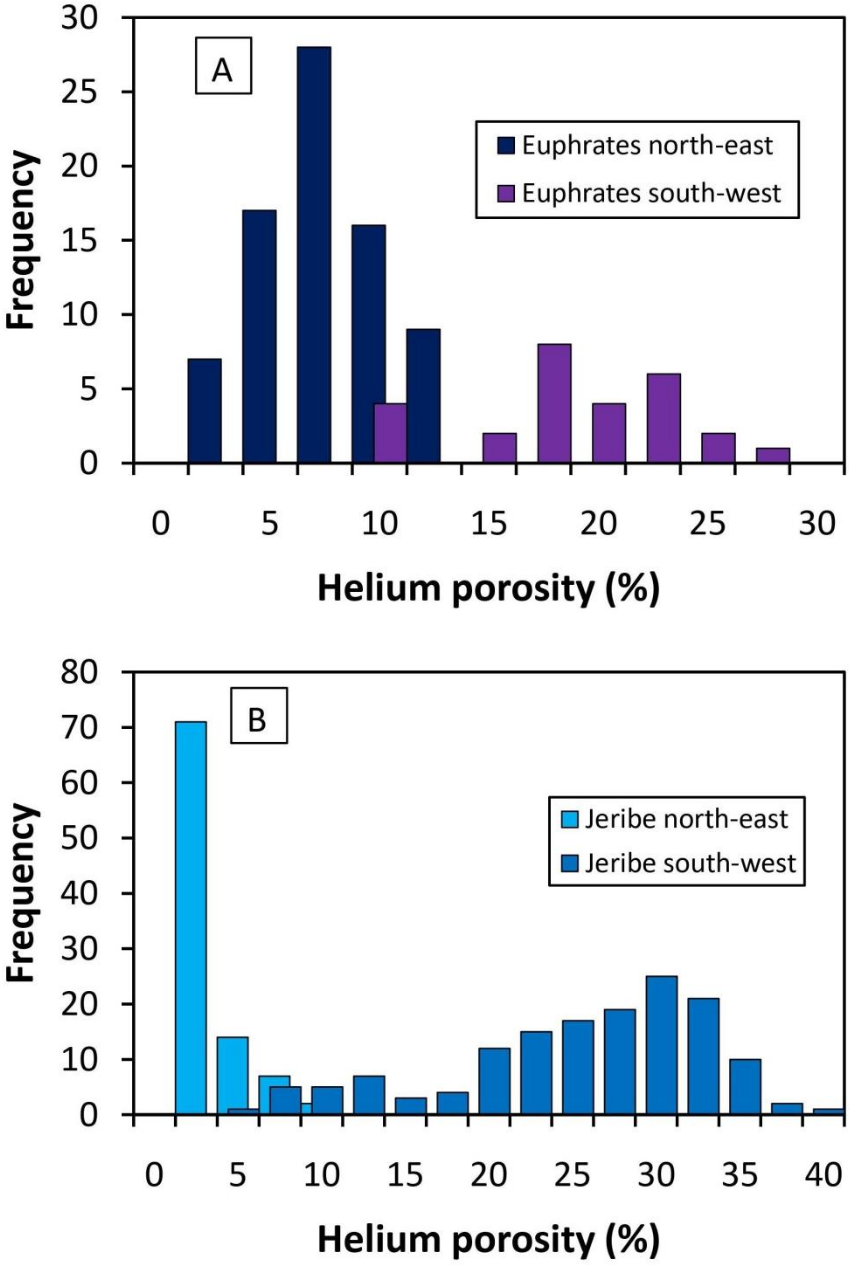

Figure 7 Frequency distribution of helium-derived porosity in the Euphrates Formation (A, *n*= 104) and the Jeribe Formation (B, *n*=240).

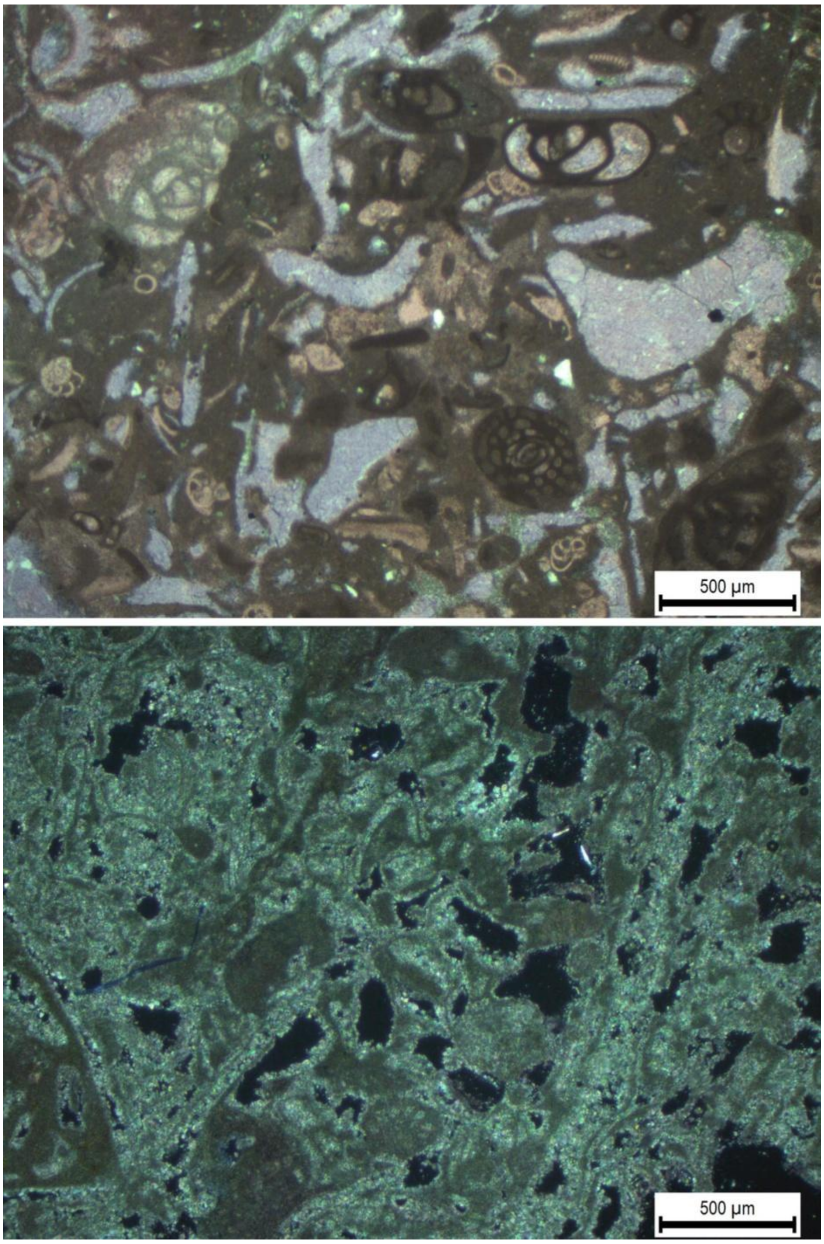

Figure 8 (1) Stained thin section from the Kormor well at a depth of 1552.30 m showing ferroan spary calcite cements filling molds and vugs, (2) Photomicrograph of stained thin section from well HR2, depth 494 m showing vuggy porosity created by dissolution, and an enlarged moldic porosity.

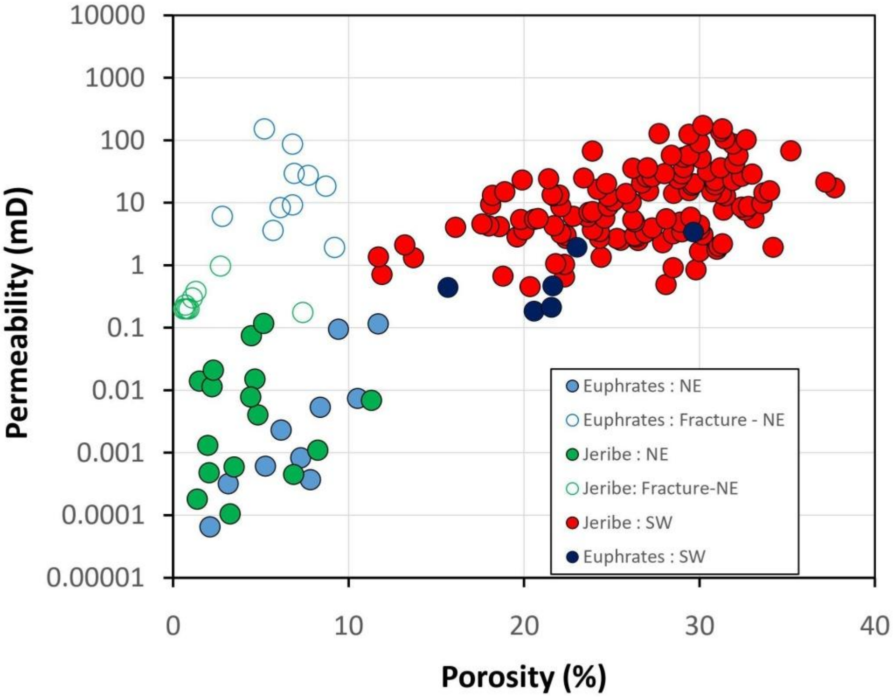

Figure 9 Poroperm cross plot showing Klinkenberg-corrected permeability as a function of helium porosity for the measured data throughout the studied area (*n*=171).

DISCUSSION

In this study lateral and vertical variations from the Lower Miocene carbonate Euphrates and Jeribe reservoir formations were determined from the NE to the SW of the study area. The different patterns of carbonate textures were identified by recognizing various microfacies from field scale observation to thin section study scale. Carbonate microfacies are characterized by diversity of bioclastic content, grain characteristics and sedimentary structures such as cross-bedding and cross-lamination. Hussein et al. (2017) identified eleven microfacies with three depositional settings in the Lower Miocene carbonate formations in the study area, which control carbonate heterogeneity and its spatial variability at a range of scales. Burial cementation has been found to greatly change the reservoir properties of coarse grainstone in the NE part of the study area, including multiphase ferroan and non-ferroan calcite cementation which has resulted in the development of variably granular mosaic, drusy, blocky and poikilotopic cement textures (Hussein et al., 2017). By contrast, early dolomitization and dissolution is interpreted to have caused a significant enhancement of the reservoir quality in the SW part of the study area.

Petrophysical variations of carbonate reservoirs are usually identified by log-based calculations and core analysis measurements (Lucia, 2007). Laboratory based petrophysical measurements show that in the north-eastern part of the study area low porosities dominate, with small pore sizes and low permeabilities, while in the south-western part of the study area high porosities and high permeabilities are generally indicated.

In this study the outcrop fracture data indicate that increased fracturing will enhance reservoir quality, especially if two different, interconnecting populations of fractures are involved. This is consistent with fracture porosities and permeabilities that have previously been identified. The recognised high intensity of fracturing in the Kurdistan region is related to tectonic activity (Rashid et al., 2019). The data in this paper allows us to hypothesize that the main factors controlling the effectiveness with which fractures enhance reservoir quality include:

1. Fracture intensity (the number of fractures per meter encountered in any direction).
2. Fracture aperture (the mean or characteristic hydraulic width of fractures).
3. Fracture occlusion (whether fractures are partially blocked by cementation or cataclasis, increasing flow tortuosity, or completely blocked).
4. Fractures mean inter-nodal distance (distance between nodes where fractures cross).
5. Fracture orientations (providing preferential directions for flow).
6. The number of fracture families based on preferential direction (where two or more families of intersecting fractures improve the inter-connectivity of the fracture network).

CONCLUSIONS

The style and quantitative expression of fractures in the Euphrates and Jeribe formations have been studied, together with the main depositional, petrophysical and microstructural properties of their host rocks.

The Euphrates Formation exhibited joints and bedding surfaces with persistence ranging between 0.3 m to over 3 m, fracture intensities of 3.3 m^{-1} and exhibited clean, rough surfaces with apertures up to 4 mm. Two distinct sub-vertical and mutually perpendicular joint sets were identified (090/81 S and 177/81 W), with the bedding orientation trending 134/05 SW.

The Jeribe Formation exhibited narrow, clean, rough joints, with persistence ranging from 0.3 m to greater than 3 m, fracture intensities of 4.35 m^{-1} and apertures up to 6.4 mm. This formation exhibits a network of two dominating fracture sets which are sub-perpendicular to each other and sub-vertical (082/81 S and 165/80 W), with the bedding orientation 134/13 SW.

Helium porosity in the north-eastern part of the Euphrates Formation ranges from 1.4±0.5% to 11.68±0.5% with an arithmetic mean of 6.36. In the south-western part of the study area the porosity is generally higher, ranging from 7.7±0.5% to 26.6±0.5% with an arithmetic mean of 17.4%.In the north-eastern part of the Jeribe Formation porosities are in the range 0.2±0.5% to 8.4±0.5%, with an arithmetic mean of 2.15%; in the south-west they are generally higher ranging from 4.4±0.5% to

37.7±0.5%, with an arithmetic mean of 24.16%. In both cases porosities are much higher in the south western region this is probably due to varying pore type and pore size distribution but are characterized by wide variation throughout the study area.

The fracture connectivity is shown to potentially enhance permeability by one order of magnitude in the Euphrates samples (3.5±0.175 mD was recorded) and up to 3 orders of magnitude in the Jeribe Formation (172.6±8.6 mD was recorded).

Acknowledgements

We express our gratitude to the Ministry of Natural Resources of Kurdistan Region and the Ministry of Oil of the Iraqi government for providing the project data.

Declarations

Conflict of interest the authors declare no competing interests.

REFERENCES

Agosta F, Kirschner DL (2003) Fluid conduits in carbonate-hosted seismogenic normal faults of central Italy. J. Geophys. Res. 108 (B4), 2221.

Agosta F, Aydin, A (2006) Architecture and deformation mechanism of a basin-bounding normal fault in Mesozoic platform carbonates, central Italy. J. Struct. Geol. 28, 1445–1467.

Agosta F, Alessandroni M, Antonellini M, Tondi E, Giorgioni M (2010) From fractures to flow: A field-based quantitative analysis of an outcropping carbonate reservoir. Tectonophysics 490, 197–213.

Ahr WM (2008) Geology of carbonate reservoirs: The identification, description, and characterization of hydrocarbon reservoirs in carbonate rocks. Canada, John Wiley & Sons, Inc., Hoboken, New Jersey, 296 P.

Al-Juboury A, Al-Tarif A, Al-Esa M (2007) Basin analysis of the Burdigalian and Early Langhian Successions, Kirkuk basin, Iraq. Geological Society, London, Special Publication, Vl. 258, P. 53-68, https://doi.org/ 10.1144/Sp285.4

Antonellini M, Tondi E, Agosta F, Aydin A, Cello G (2008) Failure modes in deep- water carbonates and their impact for fault development: Majella mountain, Central Apennines, Italy. Mar. Petrol. Geol. 25, 1074–1096.

Aqrawi AAM, Goff JC, Horbury AD, Sadooni FN (2010) The Petroleum Geology of Iraq: Scientific Press Ltd, Beaconsfield, Bucks, UK.

Awdal AH, Braathen A, Wennberg OP, Sherwani GH (2013) The characteristics of fracturen in the Shiranish Formation of The Bina Bawi Anticline; comparison with the Taq Taq field, Zagros, Kurdistan, NE Iraq. Petroleum Geoscience, V. 19, P. 139-155.

Barr D, Savory KE, Fowler SR, Arman K, Mcgarrity JP (2007) Pre-development fracture modelling in the Claire field, West of Shetland. Geological Society, London, West Of Shetland. Geological Society, London, Special Publications 270, 205–225.

Bisdom K, Bertotti G, Bezerra FH (2017) Inter-well scale natural fracture geometry and permeability variations in low-deformation carbonate rocks. J. Struct. Geol. 97, 23–36.

Buday T (1980) Regional Geology of Iraq, V. 1, Stratigraphy and Paleageography: Dg of Geological Survey and Mineral Investigation.

Croize D, Renard F, Bjorlykke K, Dysthe DK (2010) Experimental calcite dissolution under stress: evolution of grain contact microstructure during pressure solution creep. Journal of Geophysical Research-Solid Earth, Vol. 115, 1-15.

Dashti R, Rahimpour-Bonaba H, Zeinali M (2018) Fracture and mechanical stratigraphy in naturally fractured carbonate reservoirs-a case study from Zagros Region. Mar. Pet. Geol. 97, 466–479.

Dickson, J. A. D., 1965. A modified staining technique for carbonates in thin section. Nature, 205, 587.

Dickson, J. A. D., 1966. Carbonate identification and genesis as revealed by staining. Journal of Sedimentary Petrology, 36, 491-505.

Dou Q, Sun Y, Sullivan C (2011) Rock-physics-based carbonate pore type characterization and reservoir permeability heterogeneity evaluation, Upper San Andres reservoir, Permian Basin, West Texas. J. Appl. Geophys. 74 (1), 8–18.

Egermann P, Lenormand R (2005) A new methodology to evaluate the impact of localized heterogeneity on petrophysical parameters (Kr, Pc Applied To Carbonate Rocks). Society Of Petrophysicists and Well Log Analysts, SPWLA-2005-V46n5a2.

Fossen A (2016) Structural Geology. Cambridge University Press, UK, Pp 524.

Fossen H, Schultz RA, Torabi A (2011) Conditions and implications for compaction band formation in the Navajo Sandstone, Utah. Journal of Structure Geology, 33, 1477–1490.

Garland J, Neilson JE, Laubach SE, Whidden KJ (2012) Advances in carbonate exploration and reservoir analysis. In: Garland J, Neilson JE, Laubach SE, Whidden KJ (Eds.), Advances in carbonate exploration and reservoir analysis. Vol. 370. Geological Society of London, Special publication, pp. 1–15.

Grabowski G, Liu C (2010) Strontium -Isotope age dating and correlation of phanerozoic anhydrites and un-fossiliferous limestone of arabia. American Association of Petroleum Geologists, Middle East Geoscience Conference and Exhibition. Manama-Bahrain.

Graham B, Antonellini M, Aydin A (2003) Formation and growth of normal faults in carbonates within a compressive environment. Geology 31, 11-14.

Haghi AH, Chalaturnyk R, Ghobadi H (2018) The state of stress in SW Iran and implications for hydraulic fracturing of a naturally fractured carbonate reservoir. International Journal of Rock

Mechanics And Mining Sciences, Volume 105, Pages 28-43, Issn 1365-1609, https://doi.org/10.1016/J.Ijrmms.2018.03.002.

Hussein D, Collier R, Lawrence J, Rashid F, Glover PWJ, Lorinczi P, Baban DH (2017) Stratigraphic correlation and paleoenvironmental analysis of the hydrocarbon-bearing early miocene Euphrates and Jeribe formations in the Zagros folded thrust-belt. Arabian Journal of Geosciences https://doi.org/10.1007/S12517-017-3342-0.

Hussein D, Lawrence J, Rashid F, Glover PWJ, Lorinczi P (2018) Developing pore size distribution models in heterogeneous carbonates using especially nuclear magnetic resonance. Engineering in Chalk, Ice Publishing Sbn 978-0-7277-6407-2. Https://Doi.Org/10.1680/Eiccf.64072.529.

Jassim SZ, Goff JC (2006) Geology of Iraq: Dolin, Prague and Moravian Museum, Brno, Czech Republic, 341p.

Jolley S, Barr D, Walsh JJ, Knipe RJ (2007) Structurally complex reservoirs: An introduction. Geological Society, London, Special Publications, Vol. 292(1), Pp. 1–24.

Kazemi H, Merrill LS, Porterfield KL, Zeman PR (1976) numerical simulation of water-oil flow in naturally fractured reservoirs. Society of Petroleum Engineers, pp. 317–326 SPE 5719-PA.

Khoshbakht F, Azizzadeh M, Memarian H, Nourozi GH, Moallemi SA (2012) Comparison of electrical image log with core in a fractured carbonate reservoir. J. Petrol. Sci. Eng. S86–87 (3), 289–296.

Korneva I, Tondi E, Agosta F, Rustichelli A, Spina V, Bitonte R, Di Cuia R (2014) Structural properties of fractured and faulted cretaceous platform carbonates. Murge Plateau (Southern Italy), Marine and Petroleum Geology 57, 312–326.

Kosari E, Kadkhodaie A, Bahroudi A, Chehrazi A, Talebian M (2017) An integrated approach to study the impact of fractures distribution on the ilam-sarvak carbonate reservoirs: A case study from the Strait of Hormuz, The Persian Gulf. J. Petrol. Sci. Eng. 152, 104–115.

Laubach SE (2003) Practical approaches to identifying sealed and open fractures. AAPG Bulletin 87, 561–579.

Liu JZ, Sun QY, Xu GM (2008) Research on reservoir fractures in oil-gas field. Petroleum Industry Press, Beijing.

Micarelli L, Benedicto A, Invernizzi C, Saint-Bezar B, Michelot JL, Vergely P (2005) Influence of p/t conditions on the style of normal fault initiation and growth in limestones from the Se-Basin, France. J. Struct. Geol. 27 (9), 1577–1598. https://doi. org/10.1016/J.Jsg.2005.05.004.

Micarelli L, Benedicto A, Wibberley CAJ (2006) Structural evolution and permeability of normal fault zones in highly porous carbonate rocks. J. Struct. Geol. 28 (7), 1214–1227. https://doi.org/10.1016/J.Jsg.2006.03.036.

Mu LX, Zhao GL, Tian ZY (2009) Study on reservoir fracture prediction. Petroleum Industry Press, Beijing.

Nelson RA (2001) Geological analysis of naturally fractured reservoirs. Gulf professional publishing, 2nd Edition, 352 P.

Nelson RA, (1985) Geologic analysis of naturally fractured reservoirs. Gulf publishing company, Houston, Tx.

Olson JE, Dahi-Taleghani A (2009) Modeling simultaneous growth of multiple hydraulic fractures and their interaction with natural fractures. In: Proceedings SPE hydraulic fracturing technology conference and exhibition the Woodlands, Texas, USA; 2009. Paper SPE 119739.

Peacock DCP, Sanderson DJ, Rotevatn A (2018) Relationships between fractures. Journal of Structural Geology, 106, 41–53.

Rashid F, Hussein D, Lawrence J, Khanaqa P (2020) Characterization and impact on reservoir quality of fractures in the Cretaceous Qamchuqa Formation, Zagros folded belt. Marine and Petroleum Geology , 113, 104-117.

Rashid F, Glover, P.W.J., Lorinczi, P., Collier, R., Lawrence, J., 2015a. Porosity And Permeability Of Tight Carbonate Reservoir Rocks In The North Of Iraq. J. Pet. Sci. Eng. 133, 147–161.

Rashid, F., Glover PWJ, Lorinczi P, Hussein D, Collier R, Lawrence J (2015b) Permeability prediction in tight carbonate rocks using capillary pressure measurements. Mar. Pet. Geol. 68, 536–550.

Rashid F, Glover PWJ, Lorinczi P, Hussein D, Lawrence J (2017) Microstructural controls on reservoir quality in tight oil carbonate reservoir rocks. J. Pet. Sci. Eng. 156, 814–826.

Reif DB, Grasemann Faber, RH (2011) Quantative structural analysis using remote sensing data: Kurdistan, Northeast Iraq. American Association of Petroleum Geologist Bulletin, V. 95, P. 941-956.

Rustichelli A, Agosta F, Tondi E, Spina V (2013) Spacing and distribution of bed- perpendicular joints throughout layered, shallow-marine carbonates (Granada Basin, Southern Spain). Tectonophysics 582, 188–204.

Sarma P, Aziz K (2004) New transfer functions for simulation of naturally fractured reservoirs with dual porosity models. Paper SPE 90231.

Tiab D, Donaldson EC (2004) Petrophysics: Theory and practice of measuring reservoir rock and fluid transport properties. Elsevier, 926 P.

Tondi E, Rustichelli A, Cilona A, Balsamo F, Storti F, Napoli G, Renda P, Giorgioni M (2016) Hydraulic properties of fault zones in porous carbonates, examples from central and southern italy. Italian J. Geosci. 135, 68-79. https://doi. org/10.3301/Ijg.2015.08 F.1.

Van Bellen RC, Dunnington H, Wetzel R, Morton D (1959) Lexique Stratigraphique: International, Asie, Iraq. Centre National De La Recherché Scientifique, Paris P. 333.

Volatili T, Zambrano M, Cilona A, Huisman BAH, Rustichelli A, Giorgioni M, Vittori S, Tondi E (2019) From fracture analysis to flow simulations in fractured carbonates: the case study of the roman valley quarry (Majella Mountain, Italy). Marine and Petroleum Geology, Volume 100, 2019, Pages 95-110, Issn 0264-8172, https://doi.org/10.1016/J.Marpetgeo.2018.10.040.

Western Zagros (2011) Final well report of well number 1, Kurdamir Licence Block.

Yu K, Cao Y, Qiu L, Sun P (2018) The hydrocarbon generation potential and migration in an alkaline evaporite basin: the early permian fengcheng formation in the Junggar Basin, Northwestern China. Marine and Petroleum Geology, 98, 12–32.

Yuan SY, Song XM, Ran QQ (2004) Development technology of fractured reservoirs. Petroleum Industry Press, Beijing.

Zambrano M, Tondi E, Korneva I, Panza E, Agosta F, Janiseck JM, Giorgioni M (2016) Fracture properties analysis and discrete fracture network modelling of faulted tight limestones, Murge Plateau, Italy. Ital. J. Geosci. 135 (1), 55–67. https://doi.org/ 10.3301/Ijg.2014.42.

Zeng LB, Ke SZ, Liu Y (2010) Study methods of fractures in low-permeability oil-gas reservoirs. Petroleum Industry Press, Beijing.

Zhou XG, Cao CJ, Yuan JY (2003) The Research actuality and major progresses on the quantitative forecast of reservoir fractures and hydrocarbon migration law. Adv. Earth Sci. 18 (3), 398–404.

Zhou XG, Zhang LY, Fan K (2006) The research situation and progresses of natural fracture for low permeability reservoirs in oil and gas basin. Geol. Rev. 52 (6), 777–782.